Report 4/2017 • Published February 2017

OPTIMAL – Developing a decision support tool for optimization of process and product quality in fish

Izumi Sone (Nofima), Marthe J. Blikra (Nofima), Jörn Schulz (University of Stavanger) & Aberham H. Feyissa (DTU)

Nofima is a business oriented research institute working in research and development for aquaculture, fisheries and food industry in Norway.

Nofima has about 350 employees.

The main office is located in Tromsø, and the research divisions are located in Bergen, Stavanger, Sunndalsøra, Tromsø and Ås.

Company contact information:
Tel: +47 77 62 90 00
E-mail: post@nofima.no
Internet: www.nofima.no

Business reg.no.:
NO 989 278 835 VAT

Main office in Tromsø:
Muninbakken 9–13
P.O.box 6122 Langnes
NO-9291 Tromsø

Ås:
Osloveien 1
P.O.box 210
NO-1433 ÅS

Stavanger:
Måltidets hus, Richard Johnsensgate 4
P.O.box 8034
NO-4068 Stavanger

Bergen:
Kjerreidviken 16
P.O.box 1425 Oasen
NO-5844 Bergen

Sunndalsøra:
Sjølseng
NO-6600 Sunndalsøra

Alta:
Kunnskapsparken, Markedsgata 3
NO-9510 Alta

Report

Title: **OPTIMAL – Developing a decision support tool for optimization of process and product quality**	ISBN: 978-82-8296-483-8 (printed) ISBN: 978-82-8296-484-5 (pdf) ISSN 1890-579X
Tittel: OPTIMAL - Utvikling av et beslutningsstøtte verktøy for optimalisering av prosess og produktkvalitet	*Report No.:* 4/2017
	Accessibility: **Open**
Author(s)/Project manager: Izumi Sone (Nofima), Marthe J. Blikra (Nofima), Jörn Schulz (University of Stavanger) & Aberham H. Feyissa (DTU)	*Date:* 6th February 2017
Department: Processing technology	*Number of pages and appendixes:* 19+3
Client: Stiftelsen Norconserv	*Client's ref.:*
Keywords: Cod, heat- and mass transfer, modelling	*Project No.:* 11383

Summary/recommendation:

A model for coupled heat and mass transfer during baking of meat in a convection oven has previously been made using COMSOL Multi-physics. In OPTIMAL, the goal was to investigate whether the model for meat could be converted to the model for fish using data previously collected on Atlantic cod. Liquid loss, the core and surface temperature, water content, and shrinkage of the cod loin was measured and analyzed experimentally. The model was then validated by comparing the experimental and the simulated data. The project OPTIMAL was financed by Stiftelsen NorConserv. Collaboration between Nofima, DTU and University of Stavanger has been established.

Summary/recommendation in Norwegian:

Målet med OPTIMAL var å undersøke om modellen for varme- og masseoverføring under steking av kjøtt kan bli konvertert til modellen for fisk ved hjelp av eksisterende datagrunnlag på torsk. Væsketap, kjerne- og overflatetemperaturen, vanninnhold og krymping av torsk ble målt og analysert eksperimentelt. Modellen ble deretter validert ved å sammenligne de målte og simulerte verdiene. Prosjektet OPTIMAL ble finansiert av Stiftelsen Norconserv. Det ble under prosjektet etablert et samarbeid mellom Nofima, DTU og Universitetet i Stavanger.

Table of Contents

1 Background

During baking, several biochemical and mechanical processes occur as a function of temperature and time. The most prominent biochemical process is the denaturation of proteins. As a consequence of denaturation, the protein folding changes and the water holding capacity of the proteins is largely reduced. Water is thus freed inside the muscle. The free water moves towards the surface due to the presence of a concentration gradient, as well as a pressure gradient present due to shrinkage of the muscle. In meat, the liquid exudate is mainly composed of water (Feyissa et al., 2013), however in cod muscle, sarcoplasmic proteins and other non-water components make up a large part of the exudate.

The transport processes occurring during baking include heat and mass transfer. Heat is first transferred from the hot circulating air of the oven to the surface of the muscle by convection, and then from the surface to the center of the muscle mainly by conduction. A temperature gradient is quickly developed from the surface to the center, which takes much longer to heat up. Evaporation takes place when the surface temperature reaches 100 ºC. Liquid will move to the surface by pressure-driven convection, and also by diffusion due to the concentration gradient (Feyissa et al., 2013).

Liquid loss in certain fish products (especially cod) are so extensive that they must be blended in thick white sauce to "hide" the liquid loss. This is largely due to heat processing used to ensure food safety, while product quality such as mouthfeel, texture and juiciness can be compromised by excessive heat. The liquid loss is also a financial loss for the industry in terms of reduced product weight. An industry partner in a national project estimates that approximately 10-20% of their products have quality challenges associated with the liquid loss. The company estimates the total revenue loss to be NOK 36 million/year. Process optimization to ensure both food safety and product quality is often costly, time consuming and difficult. There are many variables to be considered simultaneously. Raw material, product size and shape all affect the result of processing during heat treatment. In addition, the process variables such as temperature and processing times, and combinations of these influences the product quality differently.

One possible solution is to develop a decision support tool for process optimization. The researchers at the Technical University of Denmark (DTU) (Jens Adler-Nissen and Aberham H. Feyissa) has developed such a tool for meat describing heat and mass (water) transport mechanisms during convection baking. With this tool, one can easily change the process- and product parameters (eg. cooking temperature and time) to simulate temperature development and change in water distribution in the product. In this way, time-, cost- and resource use linked to optimization can be reduced. Such a tool will also be useful for optimization of process and product quality in fish and fish products. A simulation describing when the important changes occur would be a valuable tool for the industry. This tool could both be used to select time and temperature combinations for cooking ready-meals, and in preparation of cooking suggestions for consumers when purchasing raw products. The cooking parameters could easily be optimized for cod products of varying sizes and composition of macronutrients (protein, fat, water).

The project OPTIMAL was financed by Stiftelsen NorConserv. Collaboration between Nofima, DTU and University of Stavanger has been established.

2 Materials and methods

2.1 Modelling

A 3D mathematical model of coupled heat and mass transfer describing oven roasting of meat (Feyissa *et al.,* 2013) was modified in this project for cod muscle. The model equations in Feyissa are based on a conservation of mass and energy, coupled through Darcy's equations of porous media where the water flow is mainly pressure driven.

Heat transfer within the food sample is given by:

$$c_{pm}\rho_m \frac{\partial T}{\partial t} + \nabla(-k_m \nabla T) + c_{pw}\rho_w u_w \nabla T = 0$$

where ρ_m and ρ_w are the densities of the food sample and water (kg/m^3), respectively, k_m is the thermal conductivity of meat (W/(m °C)), $c_{pm}$and c_{pw} are the heat capacities of meat and water (J/(kg °C)), respectively. u_w is the fluid (water) velocity (m/s), T is temperature (°C) and t is time (s).

Based on the conservation of mass, the governing equation for water transport within the product is given by:

$$\frac{\partial C}{\partial t} + \nabla(CU_W) = \nabla(D\nabla C)$$

where C represents the concentration (kg of water/kg of sample), t is time (s), u_w is the fluid (water) velocity (m/s) and D is the moisture diffusion coefficient (m^2/s). For meat, the value of D was set to $4 \cdot 10^{-10}$ m^2/s (Vestergaard *et al.,* 2005).

For cod, the D was set to $3.4 \cdot 10^{-10}$ m^2/s (cod, 0.05 % fat at 30 ^{o}C) (Rizvi, 1986).

According to Darcy's law of porous media, the pressure-driven fluid flow u_w inside the meat is expressed by:

$$u_w = -\frac{KE_{(T)}}{\mu_w}\nabla(C - C_{eq(T)})$$

where K is the permeability of the medium (m^2) and μ_w is the dynamic viscosity of the fluid (pa s). $C_{eq}(T)$ is the equilibrium water holding capacity as a function of temperature (T) and $E(T)$ is the modulus of elasticity (N/m^2).

The modifications made in the geometry and the thermal properties for cod muscle were based on actual measurement during validation (2.2.1 Raw material). The parameters included in Darcy's law (i.e. the water holding capacity, the elastic modulus and permeability) were modified based on the empirical data collected by Skipnes *et al.* (2011) on cod.

2.1.1 Geometry

As in meat (Figure 1), a 3D rectangular geometry corresponding to 1/4 of the original dimensions of the sample was built in COMSOL® in order to reduce the computational burden during the simulation. The geometry was built on the basis of the symmetry in the x and y directions. The original dimension of each of the 8 cod loins were recorded during validation (2.2 Validation) where the width, the length

and the height corresponded to the x, y and z coordinates, and used to build the geometry for the respective sample (see Appendix A).

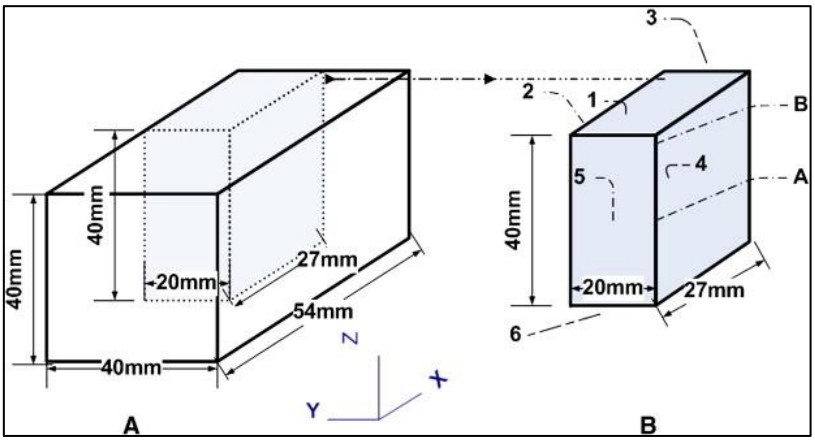

Figure 1 The geometry of the model in Feyissa et al. (2013).

2.1.2 Mesh

In Feyissa *et al.* (2013), the mesh quality was checked by running a series of simulations with increasingly finer mesh until the change in mesh density no longer had an impact on the simulation results. The generated mesh was further refined (e.g., at the boundaries where there is a high gradient) to improve the accuracy of the simulations.

Following this procedure, the model for cod was also meshed and refined at the boundary, then checked against the temperature development as well as the profile of the water distribution across the distance. For the temperature development, using the mesh finer than "Normal" in COMSOL did not improve the simulation result. However, the size of the mesh as well as the refinement of the boundary mesh affected the profile of the water distribution where the larger mesh resulted in the edgy lines (peaks) (Figure 15), instead of the smooth ones as seen in Figure 5B and 5C in Feyissa *et al.* (2013). In order to obtain the smooth lines in the model for cod, the mesh size "Finer" and the boundary layers (with thickness $2e^{-4}$) were necessary, making the computation rather heavy and impractically long. Since using the mesh size did not affect the interpretation of the result, it was decided that the mesh size Normal coupled with the refined boundary layer was adequate for the validation purpose of this project.

2.1.3 Thermal properties of cod muscle

The thermal properties of cod muscle: the density (ρ_m), specific heat capacity (C_{pm}) and thermal conductivity (k_m), were calculated based on the composition according to Rao *et al.* (2014), as in meat. The water content of the cod used for validation was measured to be 81.9 ± 0.5 %. Based on this, the protein content was assumed to account for the remaining 19 % of the muscle, while the fat and the carbohydrate were assumed to be insignificant. Skipnes *et al.* (2011) reported the composition of farmed cod muscle as water 79%; fat 0.56%; protein 20.1%; ash 1.18%. The calculated values were implemented in the equation for heat transfer and assumed constant throughout the baking.

$$\text{Density } (\rho_m) = \frac{1}{\sum \frac{y_i}{\rho_i}}$$

Specific heat capacity $(C_{pm}) = (1.6y_c + 2y_p + 2y_f + 4.2y_w) \cdot 10^3$

Thermal conductivity $(k_m) = 0.2y_p + 0.61y_w$

2.1.4 Modelling of water holding capacity (WHC)

The WHC of cod during heat treatment was determined by Skipnes *et al.* (2011) using coarsely grounded loin of farmed Atlantic cod. Heat treated samples were centrifuged (Hettich GmbH & Co. Tuttlingen, Germany) at 528 × g for 15 min at 4◦C. In this project, these data were further analyzed to create a function of WHC with respect to temperature. The maximum temperature investigated by Skipnes *et al.* (2011) was 95 °C. It was assumed that only the temperature affects the WHC, and not the treatment time in accordance to the assumption previously made for meat (Van der Sman, 2007, Feyissa *et al.,* 2013).

2.1.5 Modelling of elastic modulus (E-modulus)

Similarly, texture data produced by Skipnes *et al.* (2011) for myotomes of cod muscle was further analyzed to give a function of the E-modulus of cod. The authors used the TPA method that imitates the action of the jaw during chewing. A typical TCA curve is shown in Figure 2. Also here it was assumed that temperature only, and not time, affects the E-modulus. The E-modulus was calculated from the texture data based on Lee & Toledo (1976) as follow.

$E_{(T)}$= compressive strength/corresponding strain

$= \left(\frac{F}{A}\right) * \left(\frac{L}{\nabla L}\right)$

Where, *A* and *L* correspond to the cross sectional area and the initial length of the sample, respectively. The *A* was assumed to be identical to the areal of the compression probe (1.27 cm^2). The max force at *F* and the distance ∇L were obtained from the respective curve.

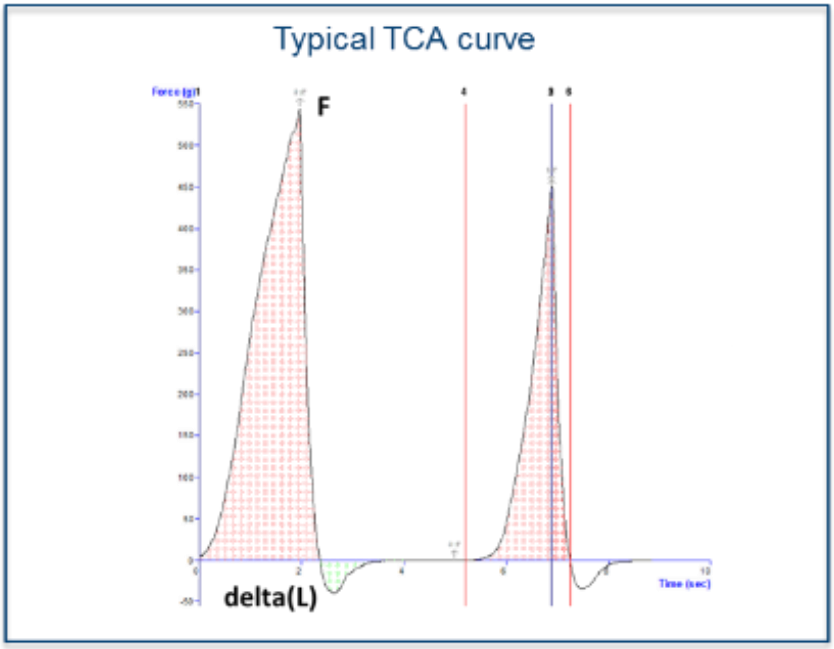

Figure 2 A typical TCA curve showing where the max force at F and the distance ∇L were obtained.

2.2 Validation

As in Feyissa *et al.* (2013), the validation aimed to: 1) validate the model for temperature development at the core and near the surface in cod muscle during baking; 2) validate the model for its ability to predict the changes in water distribution inside the sample during baking.

2.2.1 Raw material

The loins used for validation were from wild Atlantic cod, caught 11th-31st of December, 2015, using bottom trawl (norsk: bunntrål). The fish were individually packaged in plastic at Norway Seafoods, Melbu. In the production facilities, there was a temperature of 2.0-2.8 ° in the storage unit, and 3.8-4.0 °C was measured from the loins during the production. The ambient temperature during production was 13.3 °C. The fish were bought from a food store (Rema 1000) at Sunde, Stavanger, on the 24th of October, 2016, and brought to Denmark in a cooling bag with freezing elements. Still frozen, the fish were stored in a freezer at the hotel upon arrival, and brought to the Technical University of Denmark (DTU) the day after. The loins were then thawed while immersed in tap water at around 8-10 °C (Figure 3). The average water content of the loin used for validation was 81.9 ± 0.5 % (measured, N=4).

Figure 3 The cod loins during thawing.

2.2.2 Temperature validation

Cod loins (N=8) were heated in a convection oven (Combi-steamer CCC, Rational Großküchentechnik D-86899, Germany) at 150 °C for 1600 seconds (Appendix A). Temperature probes were inserted into the center of each loin, and as close as possible to the surface before baking (Figure 4). After baking, the dimensions of the fish (the length, width and height), as well as the position of the probes within the fish, were measured using a caliper (Figure 4). The measured core and surface temperatures were then compared with the values predicted from the model. In the model, the geometry was defined in accordance to the measured dimension of the fish, while the core and surface positions were corrected using the recorded position of the probes within the fish. For the core temperature, the temperature was simulated at two points: one at the position corresponding to the one recorded during the experiment, and another at the center defined by the geometry.

a b

Figure 4 Measurements of the core and surface temperature. a) The probes inserted into the loins before baking. b) Registering the position of the temperature probes after baking using a caliper.

2.2.3 Spatial distribution of water during baking

Local water was measured as described by Feyissa *et al.* (2013), after baking of cod loins (n = 2-4) for 1000 and 1600 s at 150 °C. Immediately after baking, the fish were immersed in liquid nitrogen to stop water movement inside the fish, stored in a freezer over night before transported back to Stavanger in a cooling bag with freezing elements. The samples were further stored at -18 °C until the 14th of December. To study local water distribution, ca. 2.5 cm in the middle of the loin was used. From the top to the bottom of the middle section, segments of ca. 5 mm were cut (Figure 5) and separately analyzed for the respective water content after drying at 105 °C for 16 hrs.

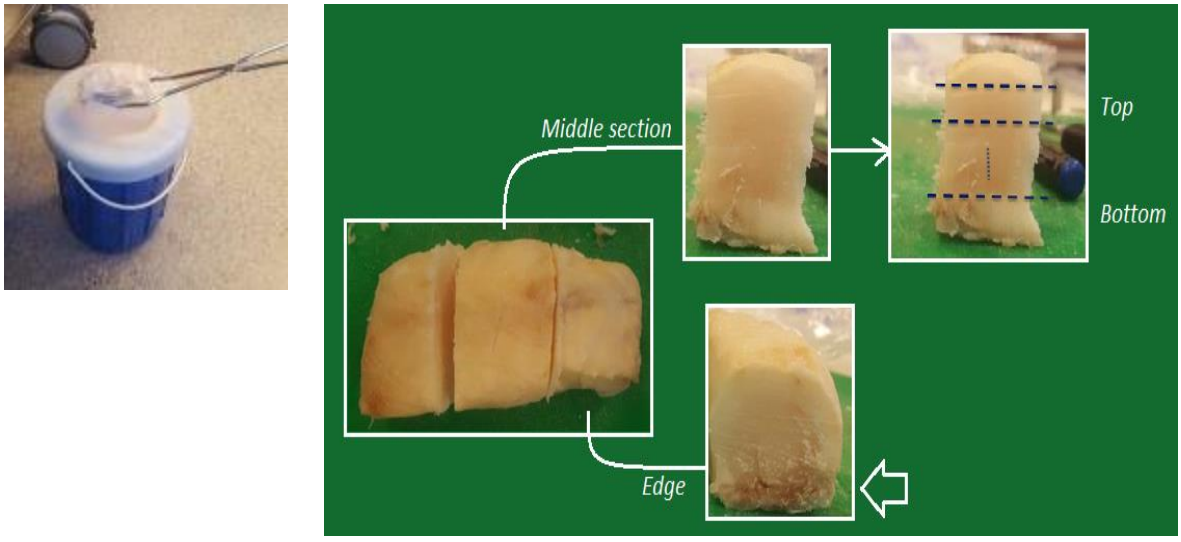

Figure 5 The slices for measurement of local water were sectioned from the top and bottom of the loin.

2.3 Additional analysis during validation

2.3.1 Weight loss

The cod loins were heat treated at 150 °C for 440, 660, 1000, and 1600 seconds, in order to reach a core temperature of 25, 40, 55 and 77 °C, respectively. The weight of the muscle before baking was noted. After baking, both the liquid (water and water-solvable small substances) and the solid (curd,

white mass in Figure 6) fraction of the exudate was collected from the baking paper and weighted separately.

a b c d

Figure 6 Measurements of liquid and curd loss from the filet during baking. a) The cod filet on baking paper after baking; b-c) the cod filet removed, showing the liquid and curd (white mass); d) the cod filet is held above the baking paper to let liquids run off to the paper.

2.3.2 Shrinkage

The heat treatment was as described in 2.3.4. The height, width, and length of cod loins were measured before and after baking at 150 °C using a caliper. When there were large differences between the maximum and minimum measurements (for instance large differences in height throughout the sample), an average of the minimum and maximum result was recorded.

3 Results and discussion

3.1 Modelling

3.1.1 WHC

The WHC was modelled by two different approaches. First by assuming a sigmoid function and second by a piecewise function combining a sigmoid function with a damped co-sinus function.

The first approach was motivated by Van der Sman (2007). For each temperature, the WHC is modeled by an exponential function time, i.e., a function of the form

$$f(x) = c + a \cdot b^x .$$

The red points in Figure 6 are the constant parameters c from the fitted exponential functions for different temperatures. The dashed red line visualizes the fitted sigmoid function based on the constant parameters. This model corresponds to the model for WHC in meat as suggested in Van der Sman (2007).

In addition, the median values are visualized in Figure 7 by the green solid points. We can observe that the median values are less influenced by outliers compared to the fitted constant parameters. Therefore, we decided to choose the median for modeling the WHC. The dashed green line correspond to a fitted sigmoid function based on the median values.

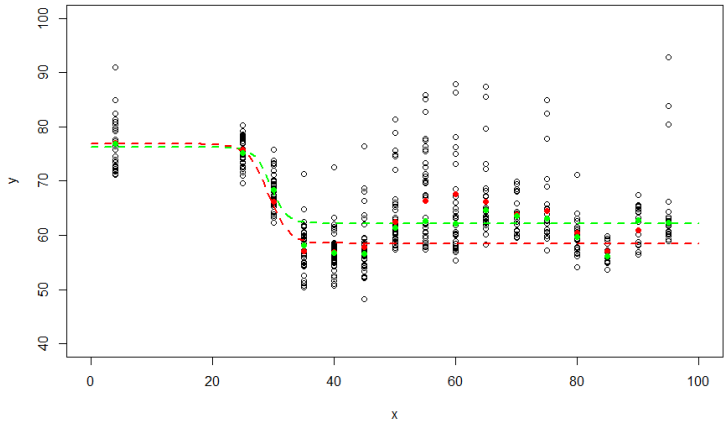

Figure 7 *WHC (y-axis) for different temperatures (x-axis) modeled by a sigmoid function based on the fitted constants from exponential functions (red points) and the median (green points).*

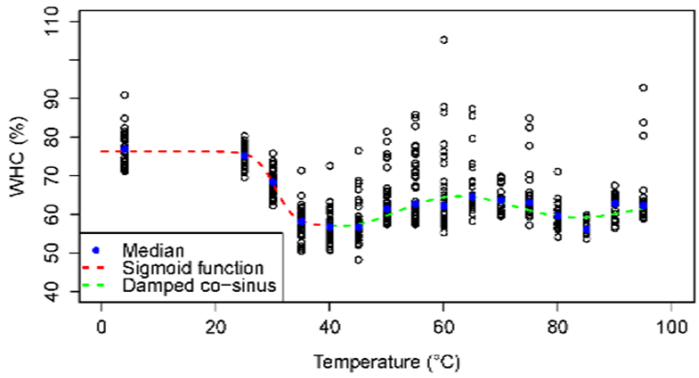

Figure 8 *Data of water holding capacity (WHC) for cod filets heat treated 10, 15, and 20 minutes (values grouped together) at temperatures from 25-95 °C.*

In contrast to WHC in meat (Van der Sman, 2007), the sigmoid function is a rather poor model for modeling WHC in fish. In particular after 40ºC the median seems to oscillate with decreasing amplitude. Therefore, a piecewise model was applied combining a sigmoid function and a damped co-sinus. This model is visualized in Figure 8.

In Figure 8, the dashed red line is a fitted sigmoid function and the dashed green line correspond to a fitted damped co-sinus based on the median values (blue solid points). In addition, the measurement are visualized by the small black circles.

An equation for WHC as a function of temperature (T) was developed for the purpose of the simulation, and is given below:

The Sigmoid function is defined by

$$S_{(x)} = A - \frac{C - A}{(1 + \exp(-G(x - T))}$$

where A = lower asymptote; C = Carrying capacity; G = Growth rate; T = time max. Using the median, the parameters were defined as follow. A = 76.31; C´ = 95.54; G = 0.60; T = 30.45.

The Damped cosines function is defined by

$$d_{(x)} = b_3 \cdot \cos(b_1 \cdot (x - b_2)) \cdot \exp(-b_4 \cdot x) + b_5$$

Using the median, the parameters were defined as b_1 =0.149; b_2 = 61.8; b_3= 10.13; b_4= 0.0123; b_5=61.5.

The WHC is modelled by

$$WHC(T) = \begin{cases} S_{(x)} \text{ if the temperature } x \text{ is } \in [0, 40] \\ d_{(x)} \text{ if the temperature } x > 40 \end{cases}$$

The WHC increases with increasing degree of protein denaturation, due to loosening of the matrix. Since increased processing temperature gives an increase in the rate of denaturation, it is expected that increased temperature decrease the WHC. However, WHC is also dependent on the time of cooking (Skipnes *et al.,* 2011), although this was not considered here. In addition, since it takes much longer for the core of the loin to reach the denaturation temperatures than the portion closer to the surface, WHC also varies with the position inside the loin. The latter should be parallel to the proportion of heat transfer.

The relationship between WHC and temperature is not straight forward. Assuming that the WHC is independent of time, a decrease of WHC can be observed between 20 and to 40C. Afterwards, we observe an oscillation of the WHC with decreasing amplitude (see Figure 8). However, given a larger data set, the inclusion of additional covariates like treatment time should be considered in the future.

3.1.2 E-modulus

Table 1 below summarizes the current data set for the corresponding temperatures.

Table 1 The descriptive summary of the data set used for modelling of the E-modulus

Temperature	Number of elements	Median	Mean	Variance	Standard error	Lower CI	Upper CI
4	20	423.9793	492.7128	72238.03	60.09910	366.9239	618.5016
30	3	951.4044	942.9335	38722.82	113.61165	454.1020	1431.7650
40	9	1642.8895	1670.8115	210519.52	152.94135	1318.1281	2023.4949
50	9	1440.9879	1347.1260	83180.78	96.13693	1125.4338	1568.8181
55	4	1077.8033	1091.9307	15263.95	61.77367	895.3393	1288.5221
60	27	1755.5513	1702.5977	674192.21	158.01924	1377.7845	2027.4109
70	11	1645.6288	1890.0494	685402.78	249.61840	1333.8650	2446.2339
80	13	1927.5309	1976.2661	1160080.79	298.72560	1325.3989	2627.1333
90	5	1726.7818	2011.5907	439356.88	296.43106	1188.5661	2834.6153

Figure 9 shows the mean elasticity over time categorized by different temperatures. The small crosses visualize each observation. Each line shows the progression of the mean elasticity for a given temperature over time. Each line starts with the same mean value at time point 0 where the elasticity is measured at a temperature of 4ºC. For several temperatures (e.g., 50, 70 and 80 ^{o}C), the lines seem constant. However, this is not the case for temperature 40 or 60 ^{o}C, for example. Further measurement would be required in order to validate the assumption that the progression of elasticity is not depend of time.

Figure 10 shows the progression of the median elasticity (in opposite to the mean in the 1st figure). In general, the median is a more robust measurement, particularly for a low sample size. However, the independence assumption of the time factor also seems to be more questionable given the current data.

Figure 11 shows the progression of elasticity for different temperatures under the assumption that time is an independent factor. Given the limited amount of data, an exponential model as shown in the blue, dotted line seems to be most suitable. The green, dotted line shows a sigmoid function. The exponential model gives better results on the residuals, but more data is required in order to do more sensitive statistical inferences.

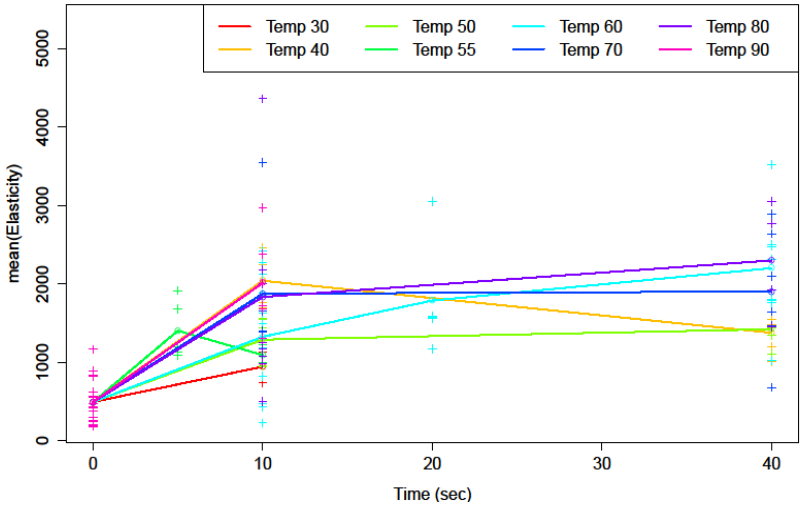

Figure 9 *The mean of the E-modulus over time categorized by different temperatures.*

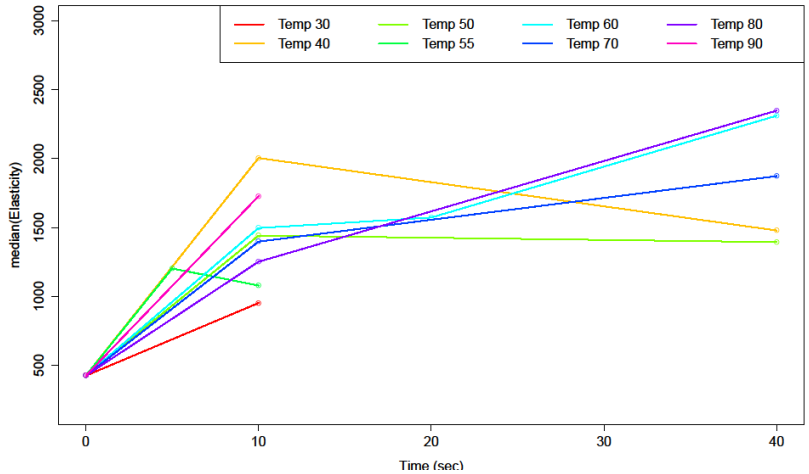

Figure 10 *The median of the E-modulus over time categorized by different temperatures.*

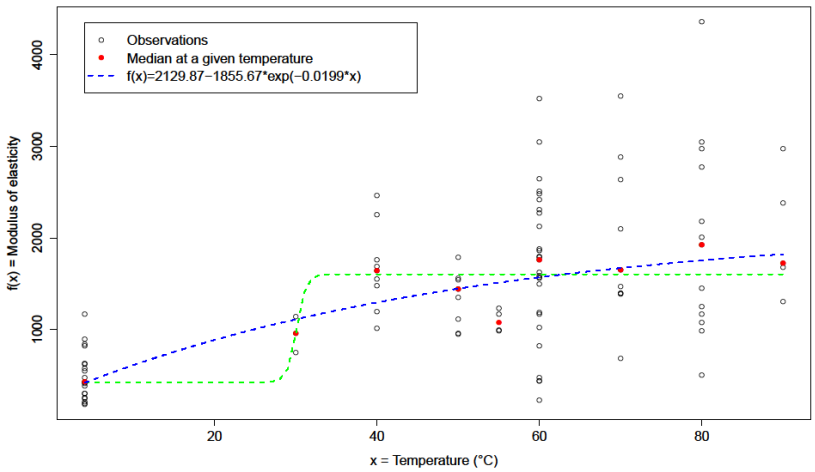

Figure 11 *The E-modulus of raw and heat treated cod myotomas plotted against temperature of heat treatment.*

An empirical relationship between E-modulus (E) and temperature (T) was formulated:

$$E(T) = 2129.87 - 1855.67 \ * \exp(-0.0199 \ * \mathrm{T})$$

The alternative Sigmoid function was obtained as

$$S_{(x)} = A \ - \ \frac{C \ - A}{(1 \ + \exp(-G(x \ - T))}$$

where A = lower asymptote; C´ = carrying capacity; G = growth rate; T = time max. The parameters were defined as follow. A = 1602.4; C´ = 1780.9; G = -1.77; T = 30.12.

The simulation results on the core temperature or the volume average of the water content in the sample seemed significantly affected by using the exponential or the Sigmoid function for the E-modulus. Based on the result on the residual, the exponential function was used for validation.

There were large standard deviations associated with the data, as seen from the wide distribution of E-modules for each temperature, especially at 60 and 80 °C. Looking at the observation (Figure 9 and Figure 10), these deviations could not be corrected enough by factoring time into the equation, as there are large difference between the values when both temperature and time is consistent. It is not known whether these deviations are due to large biological differences between and within the cod, or due to methodology. It follows that further standardizing the material or further improving the method should be explored to obtain an improved function for the change in E-modulus upon heat treatment of cod.

3.1.3 Permeability

To our knowledge, few (if at all) data is available that describe and quantify the temperature dependence of permeability of fish muscle. The available data on this parameter is also limited in case of meat, as pointed out in the paper by Feyissa *et al.* (2013). Due to the limited data, the authors used K= 10^{-17} m^2 obtained by Datta (2007) using raw meat, and the same value was also applied in the fish model. Kovácsné Oroszvári *et al.* (2006) has reported a change of 100 fold in permeability during frying of beef burger, while Feyissa et al. (2013) demonstrated the considerable effect of the permeability on the prediction of water distribution during baking by running simulation with two different values (K = 10^{-16} or 10^{-17} m^2). More quantitative knowledge of the permeability as a function of temperature for cod muscle is needed, and this will be investigated in the future project.

3.2 Validation

3.2.1 Temperature validation

Figure 12 and Figure 13 show the validation result for temperature at the center and near the surface obtained with a sample with the dimension of 54 x 85 x 27 mm (x, y, z, corresponding to the width x length x height of the sample). The measured dimensions of the remaining samples are also given in Appendix A. The initial temperature was measured to be 10.33 and 11.36 ^{o}C, respectively, and the average value of the two (10.85 ^{o}C) was used as the initial temperature for temperature simulation in the model. The measured core temperature and the simulated core temperature are very close in values and in the shape of the curve (Appendix B), as seen by the example in Figure 12.

The simulated surface temperature curve is, however, different from the measured temperature curve (Figure 13). The dotted line in Figure 13 represents the measured temperature near the surface and the blue line shows the simulated temperature at the coordinates recorded after baking. Temperature validation for this particular sample appeared to be quite good, but the deviation between the simulated and measured values were large for most of the remaining samples (Appendix C). Here the curves differ in their initial rate of increase, their limiting (highest) value, and whether or not the curve had a lag-phase (slower rate initially). These differences were not constant, but varied from sample to sample. Thus, there seems to be some challenges in determining and/or simulating the temperature when approaching the surface, where boundary conditions apply.

One possible error source, particularly for validation near the surface is the procedure used for temperature measurement. The probe was difficult to hold at the same position during baking, and the position was difficult to accurately measure following the heat treatment. The procedure for temperature measurement needs to be reviewed and revised, in order to fully examine the model's ability for temperature prediction and to identify the possible error source(s). Also note that significant shrinkage of the muscle was observed (3.3.2 Shrinkage) during baking, changing the dimension of the sample as well as the boundary conditions. This may also contribute to the deviation observed near the surface where the structural changes occur.

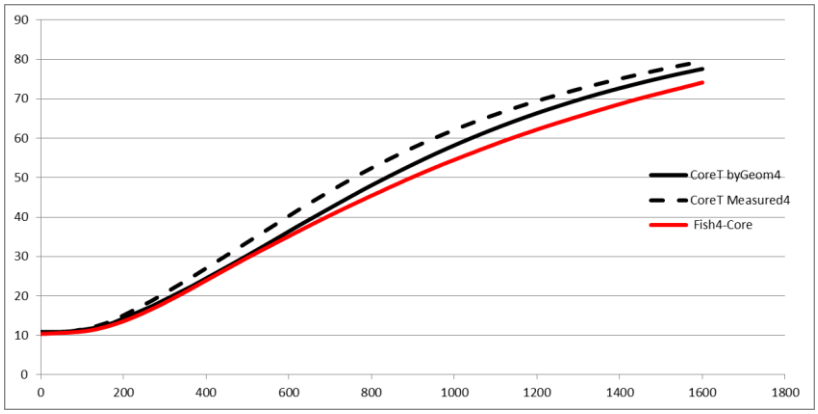

Figure 12 *Validation for the core temperature: the black, solid line (CoreT byGeom4) represents the simulated core temperature at the center, defined according to the given dimension of the sample. The red, solid line (Fish4-Core) shows the simulated temperature at the coordinates at which the probe was found. The black, dotted line (CoreT Measured4) is the measured core temperature.*

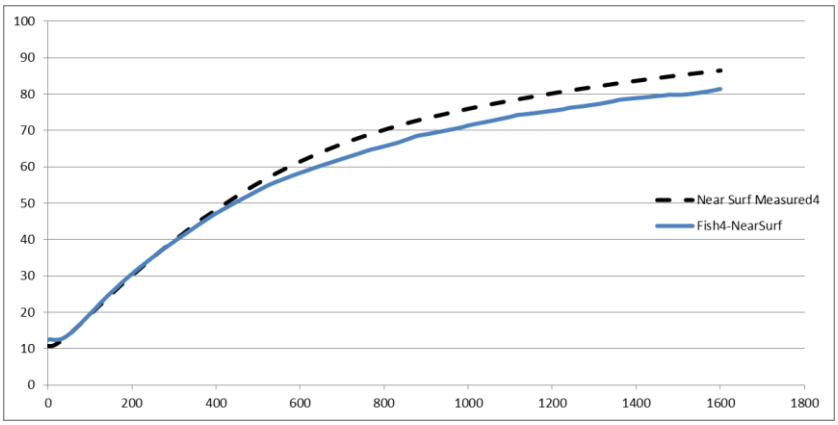

Figure 13 *Validation for the temperature near the surface. The black, dotted line (Near Surf Measured4) represents the measured temperature near the surface and the blue line (Fish4-NearSurf) shows the simulated temperature at the coordinates recorded after baking.*

3.2.2 Spatial distribution of water during baking

Table 2 shows the average water content of the segments, each prepared in ca 5 mm thickness from the top to the bottom of the middle section cut from each loin sample. The top layer of the sample at 1000 and 1600 s has the lowest water content compared to the rest of the sample, mainly because of the water evaporation from the surface. After baking for 1600s, the increased exposure time to the high temperature (150 ^{o}C) explains the lower water content at the top compared to that at 1000s.

Table 2 Measured local water content (n=2-4) from the top to the bottom of cod loin.

Time (s)/Position	1000 s	1600 s
Top	76.9 (±3.2)	71.3 (±2.6)
	78.0 (±0.4)	76.2 (±1.1)
	77.7 (±0.2)	76.3 (±0.9)
		76.3 (±1.4)
Bottom	76.1(±0.6)	76.4 (±1.4)

There were some methodological difficulties, because the method was developed for meat. It was difficult to freeze the cod loins in liquid nitrogen, and the process took much longer than what was described for meat. The time could have been reduced by increasing the size of the container with liquid nitrogen. In addition, the procedure for segmenting the sample needs to be revised and the experiment to be repeated, as the thickness of each segment was not fully standardized, therefore the uncertainty to the reliability of the data obtained.

Moreover, it seems the fish were not properly bled out, which leaves a red area where blood was accumulated, seen in Figure 5. This could be associated with the slaughtering method, which was bottom trawling. It is common that some fish die many hours before the fish are transported to the ship and slaughtered. When the fish has been dead for some time, it will not bleed out properly, and blood accumulates in the muscle. This is one of the reasons why it is important to keep in mind the slaughtering method when choosing a raw material. For the future project, the slaughtering, the handling procedure and the following frozen storage of the sample will be carefully reviewed and standardized.

Figure 14 shows the spatial distribution of water predicted after baking at 150 ^{o}C for 1600 s. Figure 15 shows the predicted profile of the water concentration (kg/kg) across the sample at 0, 1000 and 1600 s. Figure 16 shows the volume average of the water content measured and predicted at 0, 1000 and 1600 s. The three figures indicate that the model could not predict the changes in the water distribution or the content in cod during baking.

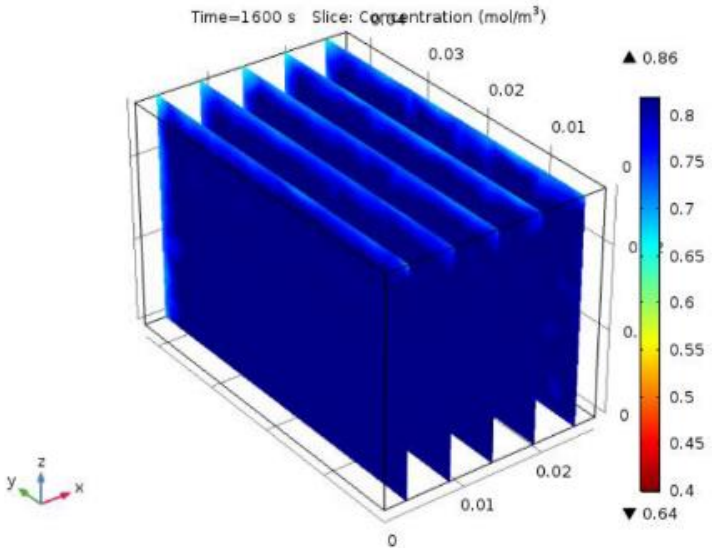

Figure 14 Simulation of the spatial distribution of water after baking at 1600 seconds

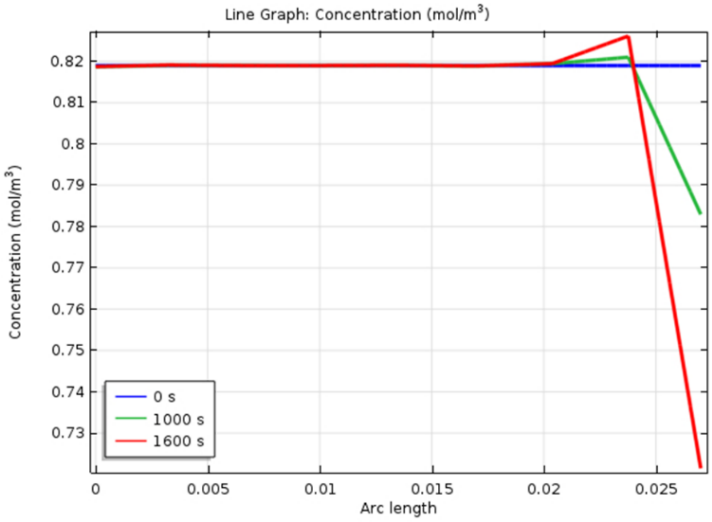

Figure 15 Temperature profile during baking as a function of the distance across the sample (Arc length) at y=0, z=height/2.

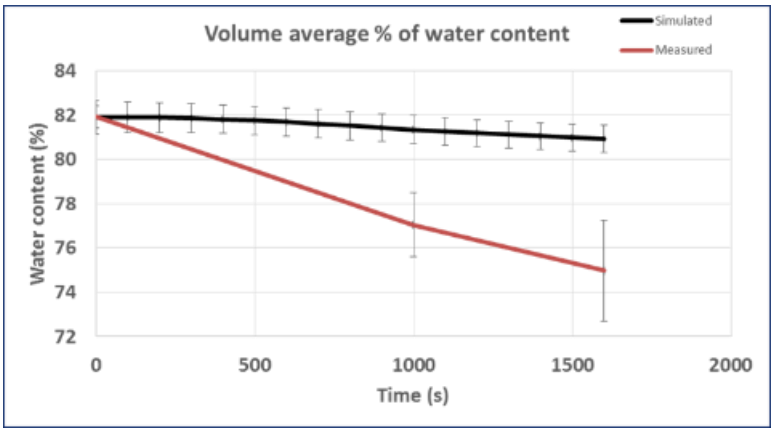

Figure 16 The average (%) of the water content simulated (N= 8) (black, solid line), compared to the measured value (in red, solid line) at 1000 and 1600s.

Possible sources for deviations are as follow. Assumption of time independence for the function of WHC, E-modulus and permeability should be reviewed and evaluated. An important question to be examined is whether and to what extent the treatment time influences the parameters such as the WHC, the E-modulus and permeability within the time frame relevant for the study. If the effect is significant, these parameters should be modelled as a function of both temperature and time.

The method used to obtain the WHC differed between Skipnes *et al.* (2011) and Bengtsson *et al.* (1976), the latter on which Feyissa *et al.* (2013) based their temperature-dependent function of the WHC for meat. Bengtsson *et al.* (1976) measured the WHC on thin slices of beef (2 mm) by immersing the sample for 10 min in water bath held constant at different temperatures. The Sigmoid function of the WHC obtained based on Bengtson et al. (1976) shows lower values of WHC at higher temperature compared to that obtained by (Skipnes *et al.*, 2011) using the centrifugation method. As the pressure-driven mass transfer is a function of $\nabla(C - C_{eq})$ where $C_{eq}$is the WHC, the low values of the WHC at higher temperature for cod may have contributed to the deviation between the simulated and the measured values characterizing the water distribution in the sample.

Another possible source for deviation concerns the E-modulus. As described above, the E-modulus for cod muscle was calculated using the texture data collected with the TPA method. The temperature-dependent function of the E-modulus implemented in the fish model was not built on the direct measurement of the E-modulus on cod muscle. This may have led to the lower values of the E-modulus obtained at higher temperature for cod muscle, but the lower value can also be attributed to the intrinsic properties of cod muscle. In the future project, the E-modulus should be directly measured.

In addition, there is a general scarcity of available data on permeability, a parameter to be included in the convective mass- and transfer according to Darcy's law. Feyissa *et al.* (2013) has demonstrated the importance of this parameter for predicting the spatial distribution of water in meat. The future project will aim to establish the data. The permeability value was kept constant in Feyissa *et al.* (2013) as well as in this project, but this assumption also needs to be reviewed.

Lastly, the model by Feyissa *et al.* (2013) assumes no flux (mass transfer) at the bottom of meat during baking (Figure 1). The same assumption was applied when developing the model for fish, but a considerable amount of liquid loss was observed at the bottom of the sample during validation. The assumption of no flux at the bottom needs to be reevaluated, as it may contribute to an overestimated value of the water content in the heat treated sample and a deviation between the simulated and measured profile of the local water distribution.

3.3 Additional analysis during validation

3.3.1 Weight loss

As seen from Figure 17, the weight loss from the cod muscle seemed to steadily increase during baking at constant temperature. The fraction which evaporated was steady at 55-60 % when baked for 7-17 minutes (440-1000 seconds), and then increased to 75 % when baked for 27 minutes (1600 seconds). Meanwhile, the fraction of the exudate as curd steadily decreased from 37 % when baked for 7 minutes, to 12 % when baked for 27 minutes. The liquid fraction of the exudate increased from 9 to 24 % when baked for 7-17 minutes, followed by a decrease to 13 % when baked for 27 minutes. The decreases in liquid and curd were parallel to the increase in evaporation during the same period.

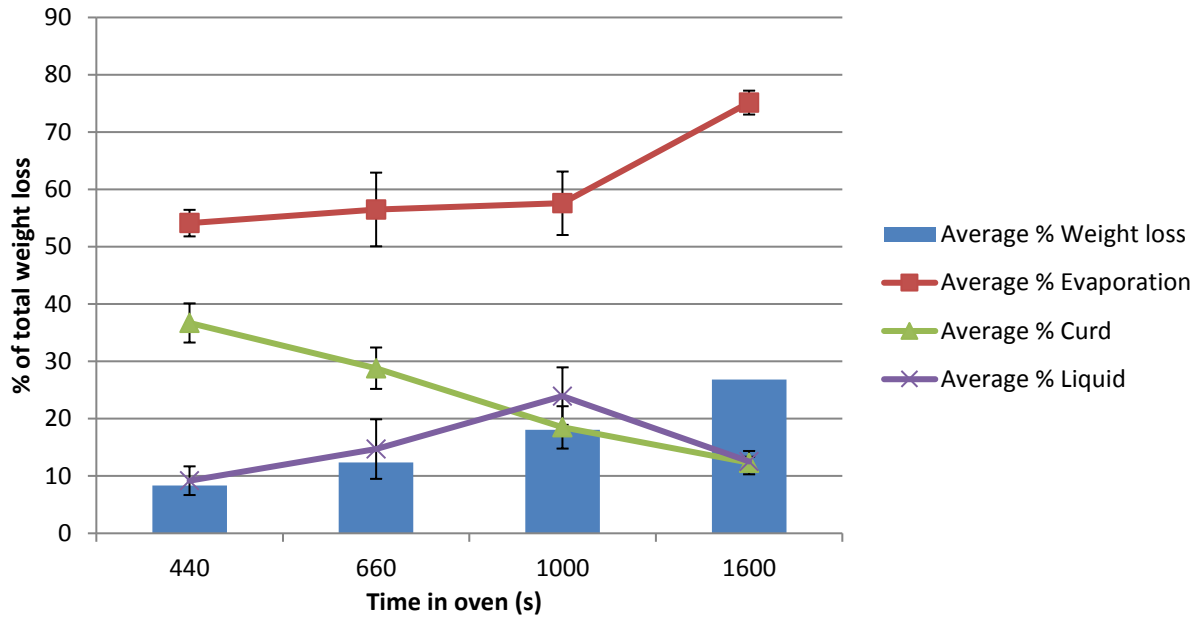

Figure 17 *Average loss of weigh, water, curd, as well as weight lost due to evaporation from cod filets baked at 150 °C for 440-1600 seconds.*

It was not investigated which components were exudated with the curd and liquid. Knowing the composition of the exudate could perhaps be advantageous, as the lost mass is substantial. Both the density and the specific heat of the material is calculated based on composition as done in meat, and if this changes significantly then perhaps they should be functions of temperature and/or time, at least with regard to water.

3.3.2 Shrinkage

There was observed significant shrinkage in at least one dimension during heat treatments (Figure 18). The shrinkage can be correlated to mass loss (at least in 2/3 dimensions), as shown in Figure 18.

.

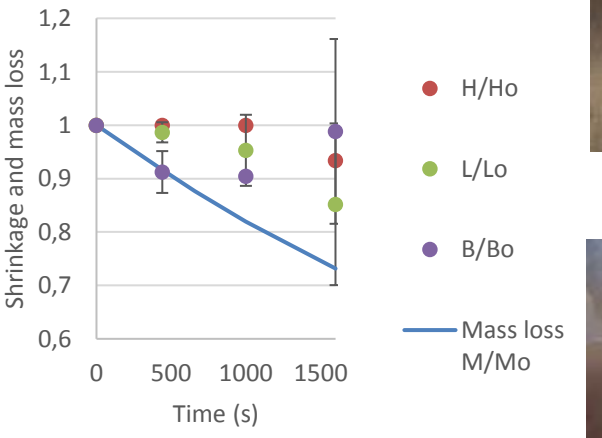

a

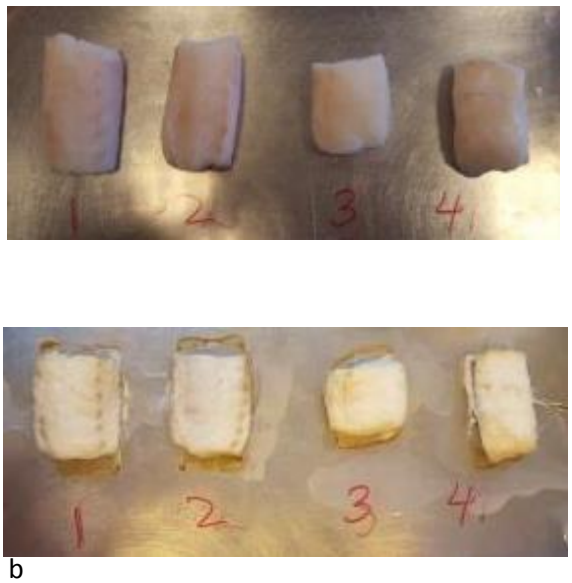

b

Figure 18 *a) Shrinkage in height (H), length (L), and width (B) as fraction of initial values plotted together with mass loss (M). b) Shrinkage of cod filets during baking at 150 °C for 1600 seconds.*

4 Conclusions

A model for coupled heat and mass transport in loins of wild Atlantic cod (*Gadus morhua*) was developed based on a simulation for meat made by Feyissa *et al.* (2013). Data acquired by *Skipnes et al.* (2011) was used for determining a relationship for the E-modulus and the WHC as functions of heat treatment temperature. The model was then validated by analyzing core and surface temperatures, the spatial distribution of water in the cod loin, and liquid loss. Shrinkage was also investigated. There was good correlation between the measured and simulated core temperatures, but there were deviations in the surface temperatures. The model could not predict the changes in the water distribution or the water content in cod during baking. The model needs further optimization in order to be a useful tool for the industry. This optimization will be carried out during OPTIMAL II.

Looking back, OPTIMAL I was a very efficient way to characterize which parameters of heat processing of cod that need further research in order to make an effective predictive model. OPTIMAL II will focus on carrying out this secondary research, during a period of 3 years. Below is a list of parameters which should be considered for further research.

- The model **geometry** which was used was a rectangle, and the shape is not representable for most cod loins. It should be debated whether it is possible (and necessary) to change the model geometry.
- **Permeability (K)** is used to calculate the moisture transport, through Darcy's law. The factor used for permeability in OPTIMAL I was based on an estimate for raw meat. It is believed that the permeability for fish muscle will be different from that of meat, and that it changes with heat treatment as the proteins denature and become porous. Therefore, it should be discussed if developing a relationship for K as a function of temperature and time (K(T,t)) would affect the accuracy of the simulation. (First, a value for K for raw, medium and thoroughly cooked cod should be found. It the values are similar, it is possible to operate with a fixed value for K.)
- Through substituting an equation for swelling pressure into Darcy's law (Feyissa *et al.*, 2013), the **E-modulus (E)** of the cod is needed. Skipnes *et al*. (2011) measured textural changes in the myotomes during heat processing by a method that simulates chewing. The data was then further analyzed to estimate the E-modulus. Changing the method and standardizing the raw material could help develop a more accurate relationship for E, either as a function of temperature only (like in OPTIMAL I) or temperature and time combined.
- **Water holding capacity (WHC)** changes with denaturation of proteins. Perhaps expressions for their denaturation rates needs to be considered in an overall expression for WHC? According to Skipnes *et al.* (2011), there is a relationship between the irregularities of WHC and E. Perhaps an expression of E(WHC) is advantageous to E(T,t)?
- The model developed in OPTIMAL I does not consider **shrinkage** of the model volume. However, the amount of shrinkage was investigated, and it was found that the shrinkage was substantial – and that it exceeds that of meat. Shrinkage is important because it exerts an additional pressure on the food, which affects the liquid transport within and out of the product. Therefore, shrinkage should be considered in the model which will be developed in OPTIMAL II, perhaps as an additional factor in the equation for pressure (Feyissa *et al.*, 2013), equation 5).

5 References

Bengtsson, N.E., B. Jakobsson & M.D. Sik (1976). Cooking of beef by oven roasting: a study of heat and mass transfer. *Journal of Food Science*, **41**:5, pp. 1047–1053.

Datta, A. (2007). Porous media approaches to studying simultaneous heat and mass transfer in food processes. I: Problem formulations. *Journal of Food Engineering,* **80**:1, pp. 80–95.

Feyissa, A.H., K.V. Gernaey & J. Adler-Nissen (2013). 3D modelling of coupled mass and heat transfer of a convection-oven roasting process. *Meat Sci.,* **93**:4, pp. 810–820.

Kovácsné Oroszvári, B., C. Sofia Rocha, I. Sjöholm & E. Tornberg (2006). Permeability and mass transfer as a function of the cooking temperature during the frying of beefburgers. *Journal of Food Engineering*, **74**:1, pp. 1–12.

Lee, C.M. & R.T. Toledo (1976). Factors affecting textural characteristics of cooked comminuted fish muscle. *Journal of Food Science,* **41**:2, pp. 391–397.

Rao, M.A., S.S. Rizvi, A.K. Datta & J. Ahmed (2014). Engineering properties of foods. CRC Press.

Rizvi, S.S. (1986). Thermodynamic properties of foods in dehydration. *Engineering properties of foods,* **2**, pp. 223–309.

Skipnes, D., S. O. Johnsen, T. Skara, M. Sivertsvik, and O. Lekang. 2011. Optimization of Heat Processing of Farmed Atlantic Cod (Gadus morhua) Muscle with Respect to Cook Loss, Water Holding Capacity, Color, and Texture. J Aquat Food Prod T 20(3):331-340.

Van der Sman, R. (2007). Moisture transport during cooking of meat: An analysis based on Flory–Rehner theory. *Meat Sci.,* **76**:4, pp. 730–738.

Vestergaard, C., J. Risum & J. Adler-Nissen (2005). 23 Na-MRI quantification of sodium and water mobility in pork during brine curing. *Meat Sci.,* **69**:4, pp. 663–672.

Appendix A

The measured dimension of the samples (cod loin) used for validation.

Fish	1	2	3	4	1-2	2-2	3-2	4-2
extern_x	58	48	56	54	52	55	53	53.5
extern_y	72	85	83	85	80	85	85	105
extern_z	29	29	27	27	33	28	29	27
extern_Px1	29	12	28.5	17	24	33	25	30
extern_Py1	36	40	31	41	37	34	34	41
extern_Pz1	15	12	15	12	18	11	18	9.6
extern_Px2	5	1	8	4.5	5.8	4.5	20	7
extern_Py2	21	40	41	48	42	30	17	30
extern_Pz2	14	15	7	14.5	19	12	13	6
extern_T_int	12.52	10.99	11.15	10.33	16.98	16.46	17.48	16.89
extern_T_int2	13.165	11.785	11.875	11.36	17.8	17.41	18.35	17.23
intial T average	12.8425	11.3875	11.5125	10.845	17.39	16.935	17.915	17.06

- extern_x, extern_y, extern_z: the width, the length and the height of the sample
- extern_x1, extern_y1, extern_z1: the coordinates where the probe for the core temperature (probe 1) was registered.
- extern_x2, extern_y2, extern_z: the coordinates where the probe for the temperature near (probe 2) the surface was registered.
- extern_T_int: the intial temperature measured at the probe 1.
- extern_T_int2: the intial temperature measured at the probe 2.
- The geometry: (x, y, z) = (extern_x/2, extern_y/2, extern_z)
- The coordinates for the center defined based on the geometry: (x, y, z) = (0, 0, extern_z/2)
- The coordinates for the centered registered during validation : (x, y, z) = (abs(extern_x/2-extern_Px1), abs(extern_y/2-extern_Py1), extern_Pz1)
- The coordinates for the temperature near the surface, measured: (x, y, z) = (abs(extern_x/2-extern_Px2), abs(extern_y/2-extern_Py2), extern_Pz2)

Appendix B

The validation results for the core temperature: The sample 1-4 to the left while the remaining 4 samples to the right. The dimension of each sample is given in Appendix A. The black, solid line represents the simulated core temperature at the center, defined according to the given dimension of the sample. The red, solid line shows the simulated temperature at the coordinates at which the probe was found. The black, dotted line is the measured core temperature.

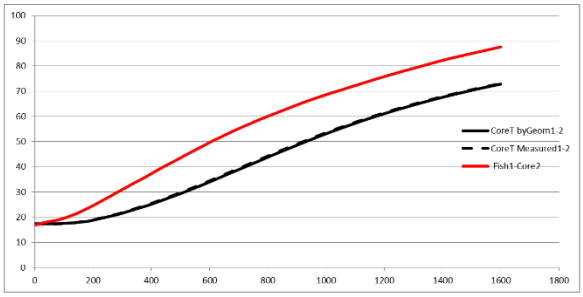

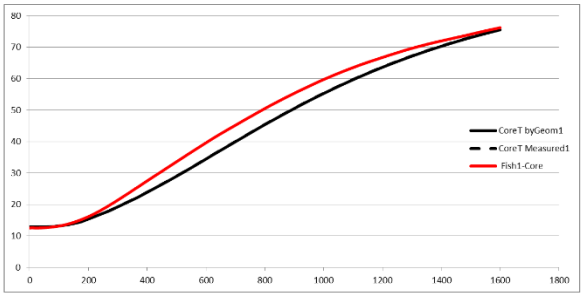

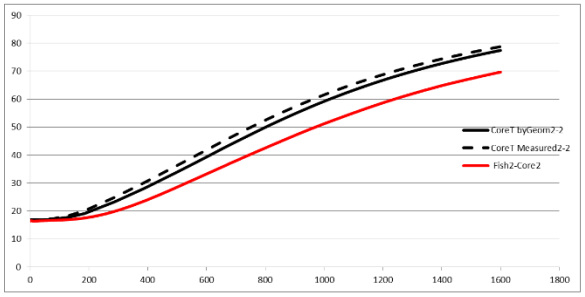

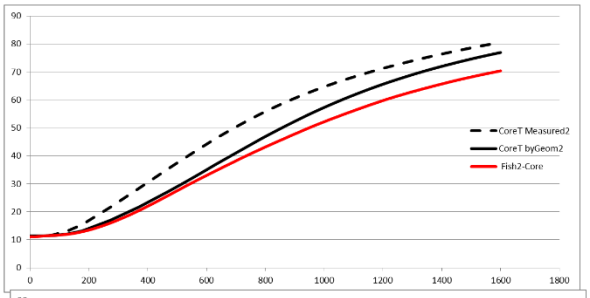

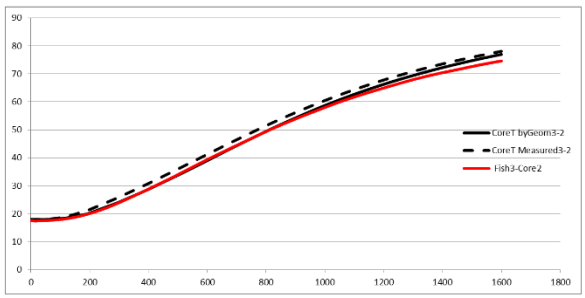

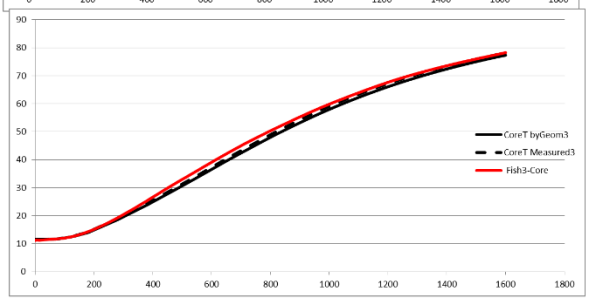

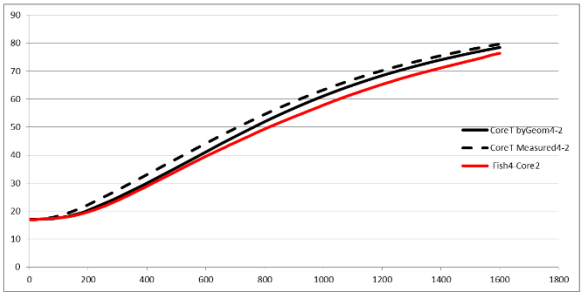

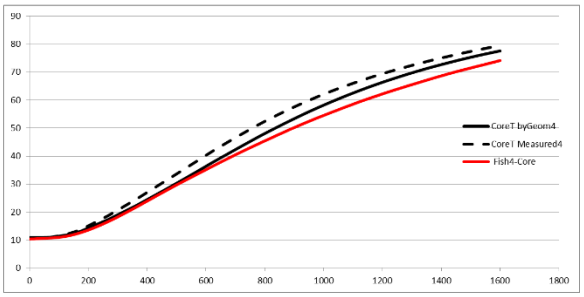

Appendix C

The validation results for the temperature near the surface: The sample 1-4 to the left while the remaining 4 samples to the right. The dimension of each sample is given in Appendix A. The black, dotted line represents the measured temperature near the surface and the blue line shows the simulated temperature at the coordinates recorded after baking.

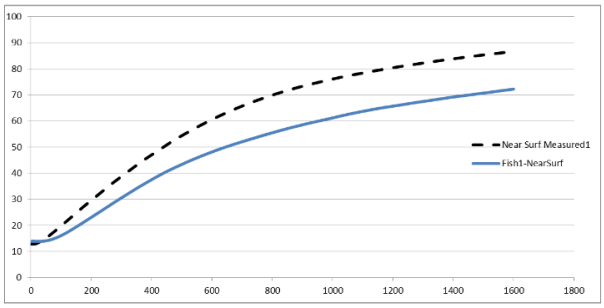

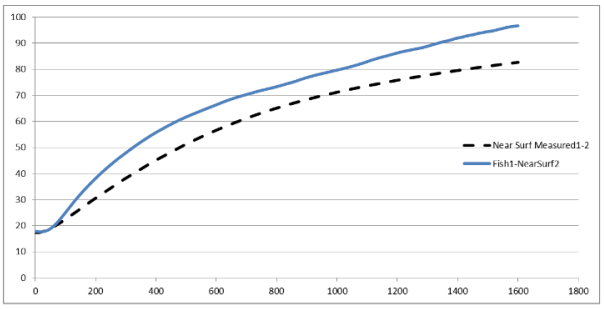

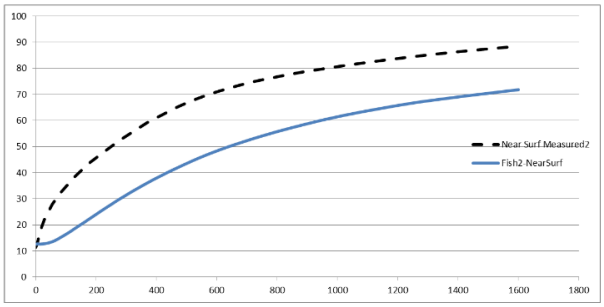

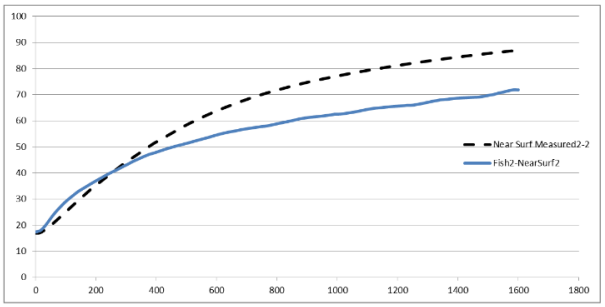

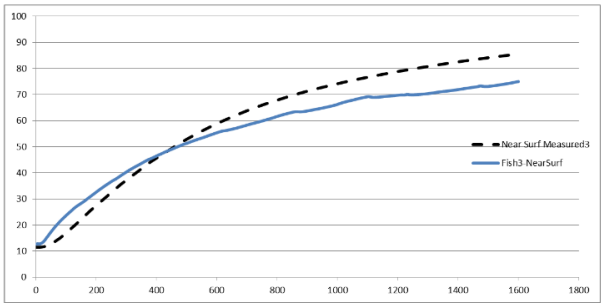

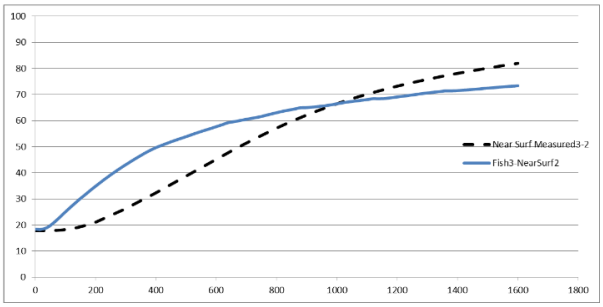

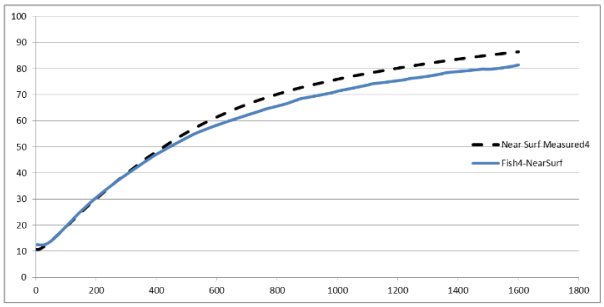

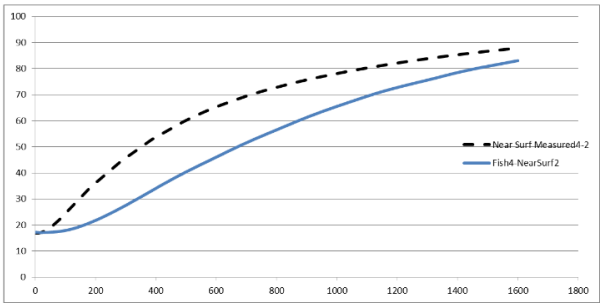

ISBN 978-82-8296-483-8 (printed)
ISBN 978-82-8296-483-5 (pdf)
ISSN 1890-579X